Rigidification of Neutral Lipid Bilayers in the Presence of Salts

Georg Pabst,* Aden Hodzic,* Janez Štrancar,† Sabine Danner,* Michael Rappolt,* and Peter Laggner*
*Institute of Biophysics and Nanosystems Research, Austrian Academy of Sciences, Graz, Austria; and †Laboratory of Biophysics, "Jožef Stefan" Institute, Ljubljana, Slovenia

ABSTRACT We studied the influence of sodium and calcium chloride on the global and local membrane properties of fluid palmitoyl-oleoyl phosphatidylcholine bilayers, applying synchrotron small-angle x-ray diffraction, spin-labeling electron paramagnetic resonance spectroscopy, and differential scanning calorimetry, as well as simultaneous density and acoustic measurements. The salt concentration was varied over a wide range from 0 to 5 M. We found that NaCl leads to a continuous swelling of the bilayers, whereas the behavior of the bilayer separation d_W in the presence of $CaCl_2$ is more complex, showing an initial large d_W value, which decreased upon further addition of salt and finally increased again in the high concentration regime. This can be understood by a change of balance between electrostatic and van der Waals interactions. We were further able to show that both salts lead to a significant increase of order within the lipid bilayer, leading to a decrease of bilayer elasticity and shift of main phase transition temperature. This effect is more pronounced for Ca^{2+}, and occurs mainly in the high salt-concentration regime. Thus, we were able to reconcile previous controversies between molecular dynamics simulations and x-ray diffraction experiments regarding the effect of salts on neutral lipid bilayers.

INTRODUCTION

Natural membranes are surrounded by an aqueous medium that contains ions such as Na^+, K^+, Ca^{2+}, Mg^{2+}, or Cl^-, and their interactions with cell membranes are known to govern processes such as gating of ion channels, membrane fusion, or phase transitions. Numerous studies on model membrane systems have demonstrated that ions have significant effects on the local and global properties of lipid bilayers (see, for example, (1–25)), and it was proposed recently that this may have important physiological implications, e.g., for synaptic transmission processes (26). Examples of locally induced changes are the change of the headgroup tilt with respect to the bilayer plane (6,20) and the ordering of hydrocarbon chains due to the formation of lipid-salt aggregates (17,18,21). In general, all observed effects are ion-specific and a function of ion size, valency, and polarizability (27), generally following the well-known Hofmeister series (for a recent review, see Kunz et al. (28)).

In this report, we focus on the effects of sodium and calcium chloride on phosphatidylcholines (PCs) in the fluid L_α phase. Monovalent salts are known to swell neutral lipid bilayers with increasing concentration (14–16,19,24,25). The prevailing understanding of this behavior is that both cations and anions bind about equally to the lipid headgroups, with reported binding constants of 0.15 M^{-1} for Na^+ and 0.20 M^{-1} for Cl^- in EggPC bilayers (7). This means, in the case of a 10-mM salt solution, that for one Na^+ ion, which is complexed with a lipid headgroup, there are ~670 lipids to which no ion is bound and that the lipid surface will be saturated with Na^+ ions at concentrations of >6.7 M salt. Likewise, one Cl^- ion will be bound per 500 free lipids at an ionic strength of 10 mM. The presence of ions leads to a change in the balance of interacting forces, which are governed, for neutral bilayers, by attractive van der Waals and repulsive hydration forces (27,29), as well as steric repulsion interactions due to membrane bending fluctuations (30). Due to the binding of ions, the bilayers are charged and additional electrostatic interactions that directly compete with long-range van der Waals interactions have to be considered. Further, van der Waals interactions are supposed to decrease in the presence of electrolytes due to screening of the low-frequency charge fluctuations (15,29). Additional complications arise because ions compete with headgroups for interfacial water, which modifies the interaction potential due to the formation of a salt-exclusion layer (22,25). Taking all these effects into account, Petrache et al. (25) were recently able to explain the observed ion-specific swelling of neutral bilayers in the presence of monovalent salts.

Compared to monovalent salts, divalent salts have a much higher binding affinity to neutral headgroups, with a reported binding constant of 40 M^{-1} for Ca^{2+} (7). Hence, one ion will be bound per ~3 free lipids in a 10-mM salt solution. This leads to significantly different bilayer interactions. At low concentrations of $MgCl_2$ and $CaCl_2$, the lipid/electrolyte system was found to swell strongly such that the multibilayer stacks break up and the system forms unilamellar vesicles (1,23). At $MgCl_2$ concentrations >10 mM, the electrostatic repulsion is progressively screened by counterions, and the system attains the same lamellar packing as in the absence of salt at an ionic strength of ~1 M. Additionally, divalent ions are known to lead to a significant upward shift of the main

Submitted May 11, 2007, and accepted for publication June 15, 2007.

Address reprint requests to Georg Pabst, Institute of Biophysics and Nanosystems Research, Austrian Academy of Sciences, Schmiedlstr. 6, A-8042 Graz, Austria. Tel.: 43-316-4120-342; Fax: 43-316-4120-390. E-mail: Georg.Pabst@oeaw.ac.at.

Editor: Thomas J. McIntosh.

0006-3495/07/10/2688/09 $2.00

doi: 10.1529/biophysj.107.112615

phase transition temperature compared to the minute effect reported in the presence of monovalent ions (31).

Besides the general consensus on the observed effects on bilayer interactions, contradictory results were published recently regarding the influence of ions on the overall structure of the bilayer. Applying all-atom molecular dynamics (MD) simulations, Böckmann and co-workers reported on the binding of Na^+ to palmitoyl-oleoyl phosphatidylcholine (POPC) bilayers with a coordination number of ~3, whereas Ca^{2+} was found to bind to around four lipid headgroups (17,21); this finding was used to explain the experimental decrease of the lateral diffusion constant (17). In addition the formation of lipid/ion clusters was reported to increase the order within the hydrocarbon chains leading to bilayer thickening. It was proposed that a maximum increase in the bilayer thickness of ~2 Å occurs in the presence of ~0.1 M Na^+. On the other hand, a detailed x-ray diffraction study in the concentration range 0–1 M salt reported no significant changes of the bilayer structure and the bending elasticity (24).

Bearing in mind that the disagreement might be due to different time- and lengthscales relevant for MD simulations compared to diffraction experiments prompted us to perform a thorough study over an extended range of ion concentrations, applying techniques that yield both local and global membrane properties, i.e., small-angle x-ray diffraction (SAXD), electron paramagnetic resonance (EPR) spectroscopy, combined dilatometric and acoustic measurements, and differential scanning calorimetry (DSC). The idea is simply that salt effects that lead to a local change of the bilayer structure eventually cause a ''detectable'' modification of the global membrane if the ion concentration is high enough. Our study is further motivated by the observed differences in bilayer interactions for mono- and divalent salts at high ionic strength. In both cases, we expect van der Waals interactions to decrease due to shielding of low-frequency contributions (25). However, swelling in this regime has thus far been observed only for monovalent ions (1,24,25). We provide evidence for a similar effect in the high Ca^{2+} concentration regime.

Regarding the effects on the bilayer structure, we found, in support of the MD results (17,21), that both salts lead to a significant increase in chain order, membrane thickness, and membrane rigidity, which is more pronounced for $CaCl_2$. These results prevail, however, only at salt concentrations larger than those studied by the simulations (>1 M). At lower concentrations, no changes to the membrane structure were observed, in agreement with previous x-ray experiments (24). Therefore, we have been able to settle the previous contradictions between the two studies.

MATERIALS AND METHODS

Sample preparation

POPC (1-palmitoyl-2-oleoyl-*sn*-glycero-3-phosphocholine, purity >99%) was purchased from Avanti Polar Lipids (Alabaster, AL) and used without further purification. NaCl and $CaCl_2$ of purity >99% were obtained from Sigma-Aldrich (St. Louis, MO). Fully hydrated multilamellar vesicles were prepared by dispersing weighted amounts of dry lipid powder in electrolyte solutions of the two salts. The ion concentration of the aqueous solution varied between 0 and 5 M. Six freeze-and-thaw cycles, using liquid nitrogen with vigorous intermittent vortex mixing, were applied, followed by a storage of the hydrated samples for 5–7 days at room temperature to ensure equilibration and equal distribution of ions. The total lipid concentration was 50 mg/ml for x-ray measurements, 5 mg/ml for dilatometric and acoustic measurements, and 20 mg/ml for DSC.

Samples for electron paramagnetic resonance spectroscopy were prepared by dissolving weighted amounts of lipid and MeFASL (3,10) spin-label in two separate organic solutions of chloroform/methanol (2:1 v/v). MeFASL was synthesized by S. Pečar (Faculty of Pharmacy, University of Ljubljana, Slovenia) and is the methyl ester of palmitic acid, where the nitroxide group is attached to the fifth carbon from the top. The stock solutions were mixed at a molar lipid/spin-label ratio of 100:1. The organic solvent was evaporated under a stream of nitrogen and, subsequently, by placing the sample under vacuum for a period of 8 h. The dry lipid films were hydrated by applying the same protocol described above with a total lipid concentration of 30 mg/ml.

X-ray diffraction

SAXD experiments were carried out at the Austrian SAXS beamline (Elettra, Trieste, Italy), using a photon energy of 8 keV and a linear one-dimensional gas detector to cover scattering vectors $q = 4\pi \sin\theta/\lambda$ from 0.01 $Å^{-1}$ to 0.6 $Å^{-1}$. Calibration of the SAXD patterns was performed using silver behenate ($d = 58.38$ Å). The lipid dispersions were poured into thin-walled quartz-glass capillaries of 1-mm diameter and placed in a homemade brass holder, which was connected to a circulation bath filled with water for temperature control. Diffraction patterns were recorded at exposure times of 2–3 min after a 10-min sample equilibration time at 300 K. Exposure times of 20 s were chosen for the temperature-resolved studies.

SAXD patterns were analyzed after background subtraction, applying the program GAP (Global Analysis Program), which is based on a previously developed global data analysis technique (32,33) reviewed recently (34). The strength of this technique is its capability to retrieve structural information from fully hydrated lamellar phases, regardless of the aggregation state (unilamellar, oligolamellar, multilamellar), applying one and the same model for the electron density profile. A meaningful comparison of the structural results among the different lamellar aggregation states can thereby be made. In this case, this is of particular importance at low concentrations of $CaCl_2$ (see below).

From the fits to the scattered intensities, we obtained the lamellar repeat distance, d, which is further subdivided into the membrane thickness, d_B, and the interstitial water layer, d_W. For d_B, we applied the definition used previously (35):

$$d_B = d_{HH} + 4\sigma_H, \tag{1}$$

where d_{HH} is the head-to-headgroup thickness and σ_H the width of the Gaussian applied to a model electron density profile of the headgroup region (32). A further parameter, directly obtained from the fit, is the Caillé parameter (36):

$$\eta = \frac{\pi k_B T}{2d^2\sqrt{K_C B}}, \tag{2}$$

from harmonic smectic theory, which is a measure for bending fluctuations that depend on the membrane bending rigidity, K_c, and the bulk modulus of interaction, B, measuring the ''stiffness'' of the interaction potential in a harmonic approximation (37). In general, bending fluctuation leads to an algebraic decay of the positional correlations that give the observed Bragg peaks a characteristic power-law decay in intensity, which is accounted for by the model function used. Finally, we calculated the lateral area per lipid from (35)

$$A = \frac{V_L - V_H}{d_C}, \tag{3}$$

where V_L is the lipid volume determined from dilatometry, V_H the headgroup volume (319 Å^3 (38)), and $d_C = d_B/2$–10 Å gives the hydrocarbon chain length.

EPR spectroscopy

EPR spectra were acquired on a Bruker ECS 106 X-Band spectrometer (Karlsruhe, Germany) under the following conditions: center field, 339 mT; sweep width, 10 mT; modulation amplitude, 0.1 mT; modulation frequency, 50 kHz; microwave power, 5 mW; scan time, 21 s; time constant, 10 ms; and receiver gain, 2×10^4. Ten spectra were accumulated for each sample to optimize the signal/noise ratio.

Because the possible formation of lipid domains due to lipid/ion interactions (14,16) leads to several superimposed EPR spectra, data were fitted within a multicomponent (multidomain) fast-restricted wobbling motion approximation using a model that allows us to distinguish up to four domains with different spectral properties (39,40). The validity of this approach, its applicability to MeFASL spin labels, and the effectiveness of the applied optimization routine have been discussed previously (39,40). In brief, the model parameters that are provided for each spectral component are the open-cone angle, ϑ, of the wobbling motion; asymmetry angle of the cone, ϕ; one effective rotational correlation time, τ_c; additional broadening constant, W; polarity correction factor, p_A; and proticity, as well as the fraction of each spectral component. It should be noted that the obtained fraction of each component in general can be different from the relative occurrence of the domains within the sample, possibly due to different partitioning coefficients of the spin label within different domains. However, the most recent experiments suggest that the partitioning coefficient for different membrane domains is very close to unity for MeFASL spin probes (41). Additionally, one has to be aware of vertical spin-probe motions. This can virtually increase the number of reported membrane domains, but can be recognized at the same time by the changes in polarity correction factors.

Due to the complex algorithms applied to find the best fitting parameters, a large number of solutions are created, which need to be condensed. This is implemented in the applied GHOST algorithm described previously (40). From the condensed set of information, we extracted the spectroscopic parameters with the highest sensitivity, which are the order parameter,

$$S_z = (\cos^2\vartheta + \cos\vartheta)/2, \tag{4}$$

and the free rotational space,

$$\Omega = \vartheta\varphi/(\pi/2)^2. \tag{5}$$

Additionally, the number and proportion of significant components (domains) are determined from the GHOST condensation procedure.

Dilatometry and velocimetry

Density and ultrasound velocity measurements were carried out using the DSA 5000 from Anton Paar (Graz, Austria), which makes it possible to perform both measurements simultaneously. The sample density is determined by measuring the oscillation frequency of a U-shaped borsilica-glass tube filled with the lipid dispersion (42). The tube is connected to an ultrasonic cell, which measures the sound velocity by evaluation of the propagation time of short acoustic pulses (frequency, 3 MHz) that are repeatedly transduced to the sample (43). Temperature control is provided by a built-in Peltier circuit. The claimed accuracy of the measured density is 10^{-6} g/ml and that of the sound velocity is <0.1 m/s. An inherent problem in measuring dispersions with the vibrating-tube technique is sedimentation or flotation, which affects the obtained values on an absolute scale. To minimize this problem, we monitored the sedimentation-induced changes in density and sound velocity at constant temperature over a period of 30 min. During this period, the corresponding values were found to change by <0.01%. Further, we repeatedly measured different samples, yielding a good overall data reproducibility. Hence, we expect that our results will be very close to absolute values.

Following the methods of others (42,44,45), we calculated the apparent partial specific lipid volume,

$$\varphi_V = \frac{1}{\rho_0}\left(1 - \frac{\rho - \rho_0}{c}\right), \tag{6}$$

from the density of the aqueous solution ρ_0 and the lipid dispersion ρ, where c is the lipid concentration. Similarly, from the sound velocity of the salt solution u_0 and u of the lipid/water system (46), we obtained the sound velocity number:

$$[u] = \frac{u - u_0}{u_0 c}. \tag{7}$$

The adiabatic compressibility of the lipid dispersion is related to ρ and the sound velocity u through the Laplace equation,

$$\kappa_s = (u^2\rho)^{-1}. \tag{8}$$

Thus, by combining the results from dilatometry and velocimetry we were able to determine the adiabatic bilayer compressibility according to (47)

$$\varphi_K = \kappa_{S0}(2\varphi_V - 2[u] - \rho_0^{-1}), \tag{9}$$

where κ_{S0} is the compressibility of the aqueous solution.

Differential scanning calorimetry

Calorimetric experiments were performed with the Microcal high-sensitivity VP-DSC (MicroCal, Northampton, MA); ~10 μl of the lipid dispersion was poured into stainless steel capillaries, which were sealed with nylon plugs and subsequently inserted into the calorimeter cell containers. The cell containers were filled with a glycerol solution to prevent freezing of the cell content.

For all samples, a scan rate of 0.5°C/min and a preequilibration time of 60 min was applied. Experiments were repeated at least twice to ensure reproducibility. Data acquisition and analysis was done using MicroCal's Origin software. The enthalpy change of the phase transition, ΔH, was obtained from the area under the peak after normalization to phospholipid concentration and baseline adjustment. The phase transition temperature was defined as the temperature at the peak maximum. All data from thermograms shown in this publication were taken from the first heating scan.

RESULTS AND DISCUSSION

All experiments were carried out at a temperature of 300 K, so that they would be directly comparable to the MD simulations by Böckmann et al. (17,21). At this temperature, fully hydrated POPC is well above the main phase transition temperature (T_m = 269.7 K, see Table 1) in the L_α phase. Fig. 1 gives an overview of the SAXD diffraction patterns obtained in the presence of NaCl and $CaCl_2$. The most significant differences occur at the lowest salt concentrations, where $CaCl_2$ induces a large swelling of the multibilayer system and d shifts from 63 Å to ~82 Å at 0.09 M. In contrast, the increase of d is almost negligible in the presence of NaCl at similar ionic strength. As the sodium chloride concentration is further increased, Bragg peaks shift slightly

TABLE 1 Main phase transition temperatures and corresponding enthalpy change of POPC in the presence of salts

Salt	x_c (M)	T_m (K)	ΔH (kJ/mol)
	0	269.7	32.8
NaCl	1	269.6	20.4
NaCl	3	270.2	15.3
NaCl	5	270.9	8.1
$CaCl_2$	1	275.8	13.3
$CaCl_2$	3	299.3	11.2
$CaCl_2$	5	299.3	6.6

to lower q values, indicating a progressive swelling also found in other systems (15,24,25). At salt concentrations >1 M, an additional peak appears in the scattering pattern between the first- and second-order reflections, indicating a phase separation reported previously in the presence of LiCl and KCl (14,16). The phase separation is most likely due to a nonhomogenous distribution of salt ions (16,24). Nevertheless, and in agreement with our previous study (16), we found that the membrane thickness of this phase is essentially the same as that of the more swollen phase. Hence, the applied global data analysis is merely affected by the presence of two phases and we were able to fit a single bilayer to the diffuse modulation of the scattered intensity (34,48). Increasing the calcium chloride concentration in turn led to a sharpening of the Bragg peaks and a concomitant shift to higher q-values. This indicates an increased scattering-domain size, as well as a decrease of the d-spacing reported previously in the presence of $MgCl_2$ (1,23). However, these studies did not go beyond a salt concentration of 1 M. At higher salt concentrations, we also found a splitting of the first-order peak in up to three different lattices (Fig. 1 *B*). We did not attempt to analyze these patterns, but the shift of the Bragg peaks and the diffuse intensity modulation clearly indicate an increase of the d-spacing and membrane thickness.

The structural results from the global data analysis are shown in Fig. 2, reporting explicitly on d in the presence of NaCl and $CaCl_2$ discussed above (Fig. 2 *A*). We first concentrate on the behavior of the membrane thickness upon increasing the salt concentration. In agreement with a previous study on the effects of halide ions (24), we found almost no increase of the membrane thickness at concentrations approaching 1 M NaCl (Fig. 2 *B*). In the range of 1–5 M salt concentration, however, d_B changed significantly. The total amount of the bilayer expansion compared to zero salt concentration is 2 Å, which agrees surprisingly well with the prediction from MD simulations (17). The effect of membrane thickening is much more pronounced for $CaCl_2$, and a rough extrapolation yields a total increase in d_B of ~6 Å at 5 M. This can only be understood if we assume that the hydrocarbon chains of POPC are almost completely stretched, as in the gel phase. Similarly, we found that the area/lipid, A, decreases more rapidly in the presence of $CaCl_2$ than in NaCl.

To find additional evidence of the x-ray results on the bilayer structure we performed EPR measurements. The spectra for pure POPC and for POPC in the presence of 5 M NaCl and 5 M $CaCl_2$ are presented in Fig. 3, and show three characteristic lines in the absence of salt. Both sodium and calcium chloride caused the appearance of an additional line at lower magnetic field values, indicating restricted motion of the spin labels. This effect is clearly more pronounced in the case of $CaCl_2$ (Fig. 3 *C*). All spectra were analyzed in

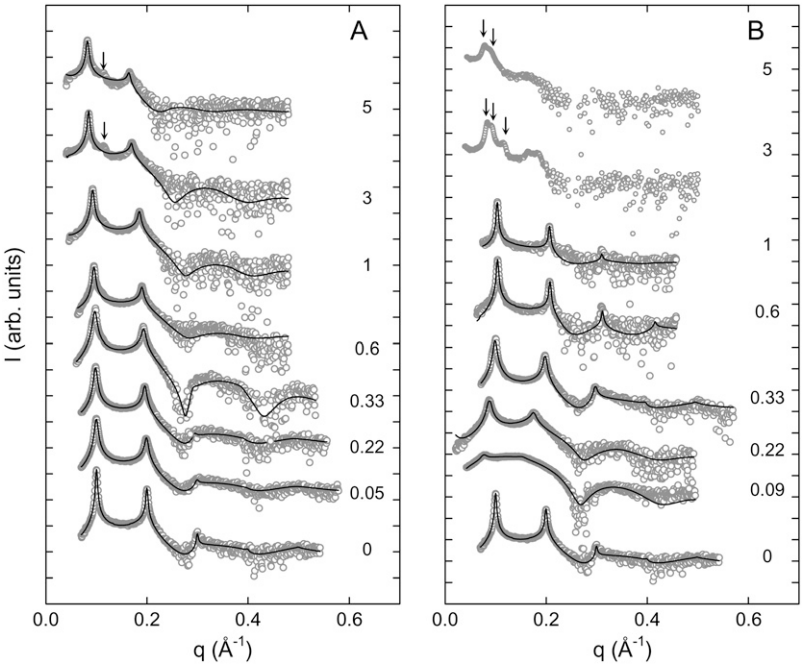

FIGURE 1 Diffraction patterns of POPC at 300 K in the presence of NaCl (*A*) and $CaCl_2$ (*B*). Numbers adjacent to the data denote the respective salt concentrations in M. Solid lines give the best fits obtained using the global analysis technique. Arrows indicate the position of additional first-order Bragg peaks due to phase separation.

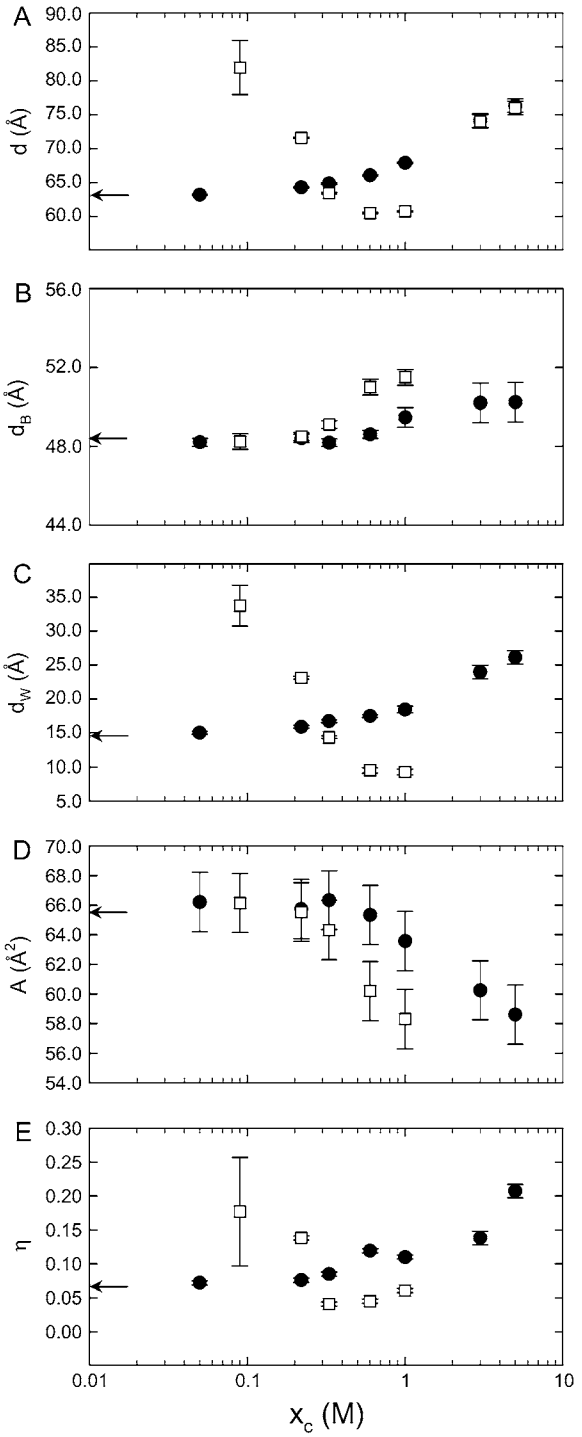

FIGURE 2 Dependence of the lamellar repeat distance (*A*), membrane thickness (*B*), bilayer separation (*C*), area/lipid (*D*), and bending fluctuations (*E*) on the concentration of NaCl (●) and $CaCl_2$ (□).

terms of the multicomponent restricted fast-motion model put forward by Štrancar and co-workers (39,40).

We found three domains of different spectral properties that are distinguished by the order parameter, i.e., with increasing anisotropy of motion. In the absence of salt, the S_z

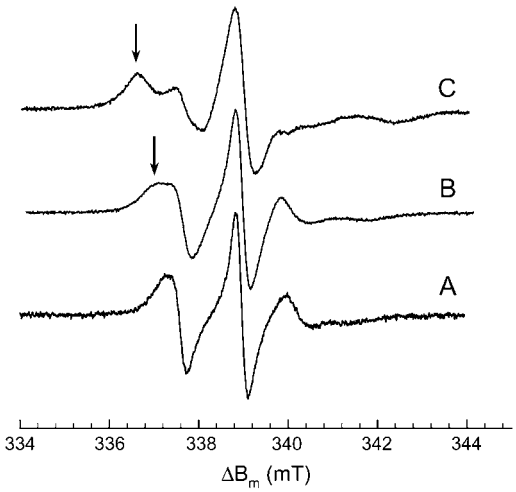

FIGURE 3 EPR spectra of POPC at 300 K without salt (*A*) and in the presence of 5 M NaCl (*B*) and 5 M $CaCl_2$ (*C*). Arrows indicate the contribution from increased restricted motions.

values are 0.43 (0.58), 0.21 (0.36), and 0.07 (0.06), where the numbers in parentheses give the fraction of each component. The corresponding polarity correction factors of 0.98, 0.97, and 0.84 indicate that the spectral component with the lowest order parameter senses a less polar environment than the other two components, most likely due to a spin probe partitioning deeper into the lipid bilayer. The most abundant component exhibited a free rotational space parameter (Ω) of 0.5, followed by 0.78, and 0.79. The full analysis of all EPR spectra revealed that the relative amount of the individual components was not significantly affected by increasing salt concentration. In particular, we were not able to detect any effect on the membrane properties in the phase-separation regime observed by SAXD (Fig. 1). All individual components showed similar relative changes as a function of ionic strength, which would not be the case if bilayers with different structures coexisted at high salt concentrations. This supports our earlier conclusion, from x-ray diffraction, that the phase splitting is due to nonuniform distribution of ions that leads to different d_Ws, whereas the membrane structure remains largely unaffected.

Because of the similar behavior of the different motional components in the presence of salts, we discuss results only for the component with the largest fraction (Fig. 4). Both NaCl and $CaCl_2$ induced a significant increase of S_z and decrease of Ω only at high concentrations. The total decrease of the anisotropic motion amounted up to ~28% for NaCl and ~77% for $CaCl_2$. Likewise, Ω decreased by ~16% in the presence of Na^+ ions and by ~60% in the case of Ca^{2+}. Hence, in agreement with our SAXD data, effects imposed by calcium are much more pronounced than those imposed by sodium.

Having discussed the properties of the local and global membrane properties, we now turn to the bilayer interactions

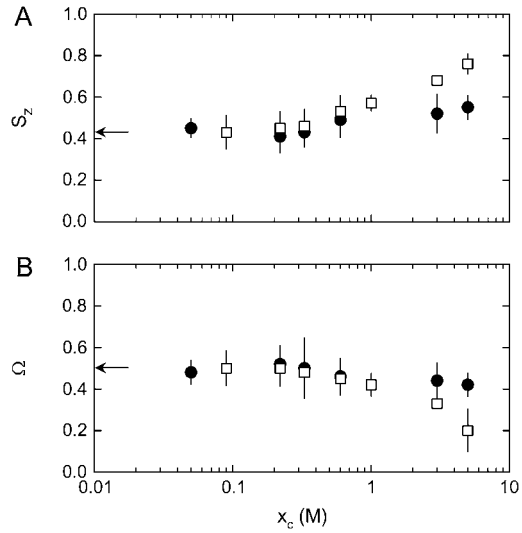

FIGURE 4 Average order parameter (*A*) and free rotational space (*B*) for POPC at 300 K as a function of NaCl (●) and $CaCl_2$ (□) concentrations. Bars indicate distribution of values obtained from the GHOST condensation technique (40).

demonstrated by the evolution of the interstitial water layer and bending fluctuations (Fig. 2, *C* and *E*). The behavior of d_W and η largely reflect the behavior for the *d*-spacing. The continuous increase of the bilayer separation is therefore understood by the interplay between a screening of the electrostatic double-layer interactions versus a decrease of the low-frequency van der Waals forces, the latter effect being especially responsible for the behavior in the high salt concentration range (25).

The evolution of d_W and η with $CaCl_2$ is even more complex. In line with (1,23), we first found an increase of the bilayer separation followed by reduction of d_W upon further addition of salt. This can be understood, at least qualitatively, in terms of Poisson-Boltzmann theory, where the strong binding affinity of Ca^{2+} ions creates already at low concentration a repulsive diffuse ion double layer. Given the binding constant of 40 M^{-1} for Ca^{2+} (7), the lipid/water interface is saturated with Ca^{2+} ions at >25 mM salt, and a progressive increase of salt leads to a concurrent increased screening effectiveness of the counterions. At 0.33 M ion concentration, the electrostatic repulsion seems to be fully screened and the structural parameters *d*, d_B, and d_W roughly correspond to the values in the absence of salt. Most interestingly, however, d_W continued to decrease as we further increased the ionic strength to the point where the space between two bilayers is reduced to ~8 Å at 1 M salt. Considering that ions will be located between the bilayers, this indicates that bilayers are basically completely dehydrated. Such behavior cannot be understood in terms of mean-field Poisson-Boltzmann theory, but can be accounted for, in principle, in terms of charge correlations that lead to significant membrane attractions in the limit of high surface charge densities and small bilayer separations (49–52). Certainly, to get a full understanding of this effect, other effects, such as ion-induced disruption of the solvent structure at the bilayer/water interface, must also be considered. However, that is not the scope of this article. Nevertheless we note that this is, to the best of our knowledge, the first observation of such an effect in a pure phospholipid system. Finally, at high ionic strength, our x-ray data from this study do not allow us to obtain a value for the bilayer separation (Fig. 1 *B*). However, there is a large increase of *d* at 3 and 5 M $CaCl_2$ (Fig. 2), which has to be dominated by swelling, since it is not realistic that d_B increases by ~15 Å in the concentration range of 1–5 M. Consequently, also, η will increase at high $CaCl_2$ concentrations.

These observations are by no means trivial to interpret, since the reason for the increase of d_W might be related to a decrease of bending rigidity, leading to increased steric repulsion of Helfrich type (30), screening of van der Waals interactions, or a combination of both. The bending rigidity can be determined from diffraction data by sensing the bilayer interaction potential through the application of external, osmotic pressure (35,53,54), or by studying the diffuse (nonspecular) intensity of aligned lipid samples (55,56). Here, we chose a different approach.

Measuring the specific lipid volume and the sound velocity also opens a window on the bulk bilayer elasticity that has been applied previously to lipid/water systems (44,45). Fig. 5 *A* shows the results for the density and acoustic measurements. Our result of 0.989 ml/g for φ_v in the absence of salt agrees with previously published data on POPC (44,57). This value remained practically constant for both salts up to a concentration of 1 M and decreased upon further addition of salt. At the same time, we found that the sound velocity number drops (Fig. 5 *B*) and the specific adiabatic compressibility decreases for both salts as the concentration is increased (Fig. 5 *C*). Sound velocity measurements on lipid bilayers have been employed previously to address the bilayer elasticity and dynamic behavior if the absorption per wavelength is monitored at the same time (44,45,58–63). In this study, we found that both salts lead to a rigidification of the bilayers. The effect is again more pronounced for $CaCl_2$, in agreement with our results from SAXD and EPR spectroscopy.

An independent check on the capability of salts to increase order in neutral bilayers can be performed by DSC. Fig. 6 *A* shows the heat capacity curves of POPC in pure water and in the presence of 1 M, 3 M, and 5 M NaCl. Corresponding thermograms in the presence of $CaCl_2$ are shown in Fig. 6 *B*. Table 1 reports the derived transition temperatures and enthalpy changes. In the absence of salt, the T_m of POPC is at ~269.7 K, in agreement with the value reported by Böckmann et al. (17), although our found enthalpy change, $\Delta H = 32.8$ kJ/mol, is somewhat larger than theirs. The addition of salt led to an increase of the main transition temperature and decrease of ΔH. In the case of NaCl, the

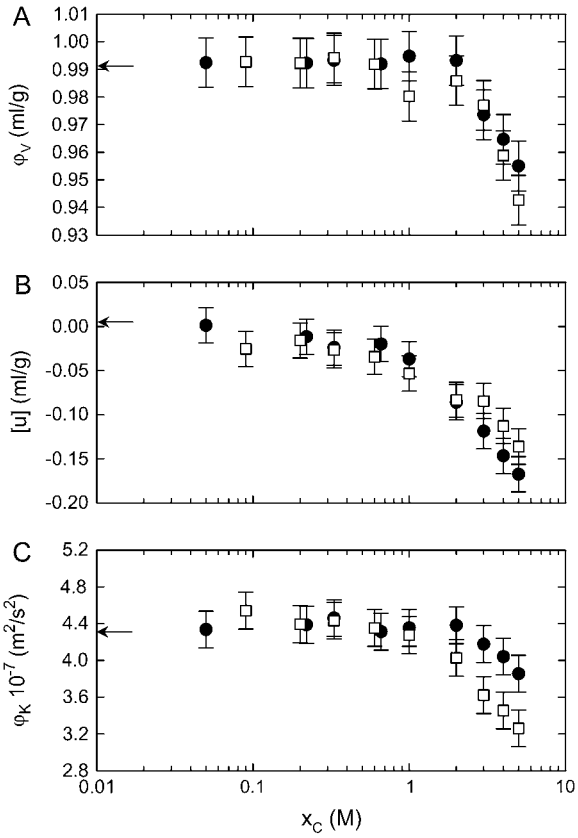

FIGURE 5 Dependence of the specific volume (*A*), sound velocity number (*B*), and specific adiabatic compressibility (*C*) on the concentrations of NaCl (●) and $CaCl_2$ (□).

maximum T_m shift occurring at 5 M salt was 1.2 K. In the case of $CaCl_2$, this effect is much more pronounced, amounting to $\Delta T_m = 29.6$ K at 3 M and 5 M salt (Table 1). This means that the measurements were performed just above the main transition in the case of 3 M and 5 M $CaCl_2$. It is well known that the bending rigidity of bilayers below the T_m is significantly higher compared to the fluid phase (64,65). Thus, DSC results also support our previous conclusions on the rigidification of POPC in the presence of salts.

On the other hand, it is also well known that increased density fluctuations in the vicinity of the main phase transition in some PCs lead to a decrease of the bending rigidity that manifests itself through an increase of the *d*-spacing upon approaching the T_m from above, commonly known as ''anomalous swelling'' (see, e.g., (35) and references therein). Thus, in principle, it might be possible that the shift of T_m in the presence of salts brings the system into the transition regime, where the bilayers experience an increase of flexibility, especially in the case of 3 M and 5 M $CaCl_2$, where the data have been obtained just above the T_m (Fig. 6). We have therefore performed SAXD experiments combined with a temperature scan (heating rate, 1°C/min) for the 3 M and 5 M $CaCl_2$ samples. The results presented in Fig. 7 show no anomalous swelling behavior of *d* in the vicinity of the

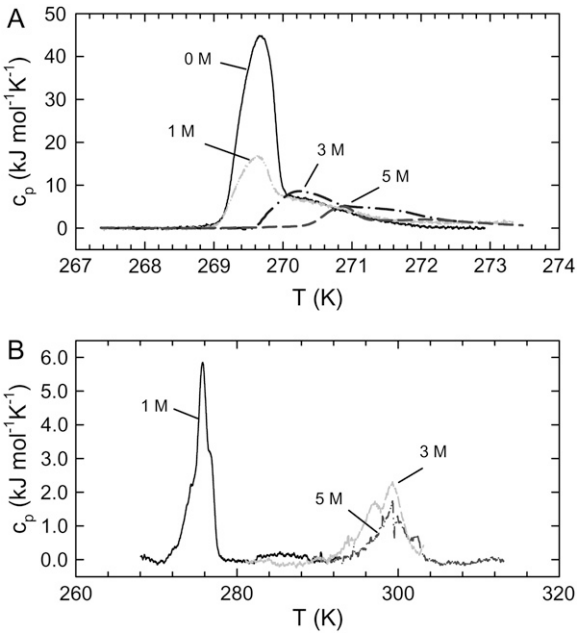

FIGURE 6 (*A*) Heat capacity of POPC in pure water and in the presence of 1 M, 3 M, and 5 M NaCl. (*B*) Thermograms obtained in the presence of 1 M, 3 M, and 5 M $CaCl_2$. Transition temperatures are summarized in Table 1.

main phase transition. Hence, we can exclude the occurrence of a drop in bending rigidity even at the highest Ca^{2+} content, in agreement with the adiabatic compressibility data (Fig. 5). Consequently, the increase of the *d*-spacing has to come from a screening of the low-frequency contributions to van der Waals interactions, as in the case of monovalent ions (25).

CONCLUSIONS

Using five experimental techniques, we have provided evidence that monovalent and divalent salts lead to a modification of the global membrane structure and elasticity. In

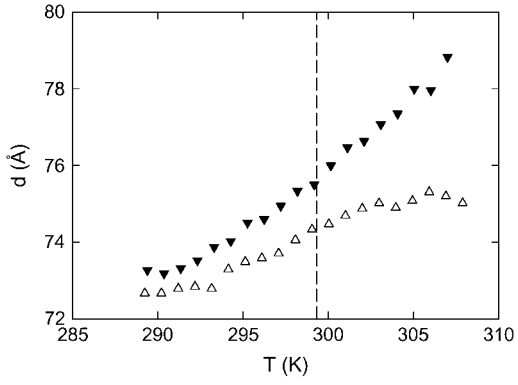

FIGURE 7 Temperature dependence of the d-spacing of POPC in the presence of 3 M (△) and 5 M $CaCl_2$ (▼). The dashed line indicates the T_m for both salt solutions observed by DSC (Fig. 6 and Table 1).

addition, salts strongly affect bilayer interactions, and all effects are in general much more pronounced for $CaCl_2$ than for NaCl, which can be attributed to their different binding affinities (7). In agreement with previous reports, we found a progressive increase of bilayer separation for Na^+, whereas Ca^{2+} causes a large swelling of the multilamellar system at low concentrations (24), which is progressively reduced with salt concentration due to electrostatic screening (1,23). Moreover, we observed a hitherto unknown regime of attraction between the chargelike membranes at $CaCl_2$ concentrations between 0.33 M and 3 M, where the membrane became almost completely dehydrated. At higher Ca^{2+} concentrations, the bilayer separation increased again, which can be explained by a decrease in van der Waals interactions, analogous to the case of monovalent ions (25).

With regard to membrane structure, the total increase of the bilayer thickness in the case of NaCl amounts to 2 Å, in surprisingly excellent agreement with predictions from MD simulations (17). However, the thickening occurs at much higher concentrations than predicted by the simulations. The most likely explanation for this partial disagreement is that the thickening effect may occur first only on a local and time-restricted level, involving some small patches of the lipid bilayer, whose contribution to the total signal gets smeared out in measurements of the sample average. Thus, such effects will be observed only above a certain threshold concentration of salt, depending on the sensitivity of the experimental technique. This explains also the controversy between the x-ray and MD studies (17,24). In agreement with Petrache et al. (24), we found no significant salt effects on the bilayer structure for ion concentrations up to 1 M. With respect to the biological significance of this study, we note that 5-M salt solutions are certainly far from being physiologically relevant. However, the electrolytic environment of biological membranes is also definitely not similar to a static and average distribution of ions. It may vary transiently very significantly on the local level. Yet, in the absence of an experimental technique that can study the structural properties of small, isolated supramolecular patches, one has to resort to methods that yield properties of the sample average. Consequently, our results are physiologically relevant, but only on a local scale.

We thank Dmitry Kharakoz for helpful discussions.

This work was supported by the Austrian Science Fund (grant P17112-B0 to G.P.).

REFERENCES

1. Inoko, Y., T. Yamaguchi, K. Furuya, and T. Mitsui. 1975. Effects of cations on dipalmitoyl phosphatidylcholine/cholesterol/water systems. *Biochim. Biophys. Acta.* 413:24–32.
2. Lis, L. J., W. T. Lis, V. A. Parsegian, and R. P. Rand. 1981. Adsorption of divalent cations to a variety of phosphatidylcholine bilayers. *Biochemistry.* 20:1771–1777.
3. Lis, L. J., V. A. Parsegian, and R. P. Rand. 1981. Binding of divalent cations of dipalmitoylphosphatidylcholine bilayers and its effect on bilayer interaction. *Biochemistry.* 20:1761–1770.
4. Cunningham, B. A., and L. J. Lis. 1986. Thiocyanate and bromide ions influence the bilayer structural parameters of phosphatidylcholine bilayers. *Biochim. Biophys. Acta.* 861:237–242.
5. Cunningham, B. A., J. E. Shimotake, W. Tamura-Lis, T. Mastran, W. M. Kwok, J. W. Kauffman, and L. J. Lis. 1986. The influence of ion species on phosphatidylcholine bilayer structure and packing. *Chem. Phys. Lipids.* 39:135–143.
6. Seelig, J., P. M. Macdonald, and P. G. Scherer. 1987. Phospholipid head groups as sensors of electric charge in membranes. *Biochemistry.* 26:7535–7541.
7. Tatulian, S. A. 1987. Binding of alkaline-earth metal cations and some anions to phosphatidylcholine liposomes. *Eur. J. Biochem.* 170: 413–420.
8. Macdonald, P. M., and J. Seelig. 1988. Anion binding to neutral and positively charged lipid membranes. *Biochemistry.* 27:6769–6775.
9. Cunningham, B. A., E. Gelerinter, and L. J. Lis. 1988. Monovalent ion-phosphatidylcholine interactions: an electron paramagnetic resonance study. *Chem. Phys. Lipids.* 46:205–211.
10. Cunningham, B. A., and L. J. Lis. 1989. Interactive forces between phosphatidylcholine bilayers in monovalent salt solutions. *J. Colloid Interface Sci.* 128:15–25.
11. Roux, M., and M. Bloom. 1990. Ca2+, Mg2+, Li+, Na+, and K+ distributions in the headgroup region of binary membranes of phosphatidylcholine and phosphatidylserine as seen by deuterium NMR. *Biochemistry.* 29:7077–7089.
12. Rydall, J. R., and P. M. Macdonald. 1992. Investigation of anion binding to neutral lipid membranes using 2H NMR. *Biochemistry.* 31:1092–1099.
13. Pressl, K., K. Jørgensen, and P. Laggner. 1997. Characterization of the sub-main-transition in distearoylphosphatidylcholine studied by simultaneous small- and wide-angle X-ray diffraction. *Biochim. Biophys. Acta.* 1325:1–7.
14. Rappolt, M., K. Pressl, G. Pabst, and P. Laggner. 1998. Lα-phase separation in phosphatidylcholine-water systems induced by alkali chlorides. *Biochim. Biophys. Acta.* 1372:389–393.
15. Korreman, S. S., and D. Posselt. 2001. Modification of anomalous swelling in multilamellar vesicles induced by alkali halide salts. *Eur. Biophys. J.* 30:121–128.
16. Rappolt, M., G. Pabst, H. Amenitsch, and P. Laggner. 2001. Salt-induced phase separation in the liquid crystalline phase of phosphatidylcholines. *Colloids and Surfaces A.* 183–185:171–181.
17. Böckmann, R. A., A. Hac, T. Heimburg, and H. Grubmüller. 2003. Effect of sodium chloride on a lipid bilayer. *Biophys. J.* 85:1647–1655.
18. Pandit, S. A., D. Bostick, and M. L. Berkowitz. 2003. Molecular dynamics simulation of a dipalmitoylphosphatidylcholine bilayer with NaCl. *Biophys. J.* 84:3743–3750.
19. Amenitsch, H., M. Rappolt, C. V. Teixeira, M. Majerowicz, and P. Laggner. 2004. In situ sensing of salinity in oriented lipid multilayers by surface X-ray scattering. *Langmuir.* 20:4621–4628.
20. Sachs, J. N., H. Nanda, H. I. Petrache, and T. B. Woolf. 2004. Changes in phosphatidylcholine headgroup tilt and water order induced by monovalent salts: molecular dynamics simulations. *Biophys. J.* 86: 3772–3782.
21. Böckmann, R. A., and H. Grubmüller. 2004. Multistep binding of divalent cations to phospholipid bilayers: a molecular dynamics study. *Angew. Chem. Int. Ed. Engl.* 43:1021–1024.
22. Petrache, H. I., I. Kimchi, D. Harries, and V. A. Parsegian. 2005. Measured depletion of ions at the biomembrane interface. *J. Am. Chem. Soc.* 127:11546–11547.
23. Yamada, N. L., H. Seto, T. Takeda, M. Naga, Y. Kawabata, and K. Inoue. 2005. SAXS, SANS and NSE studies on ''unbound state'' in DPPC/water/CaCl2 system. *J. Phys. Soc. Jpn.* 74:2853–2859.

24. Petrache, H. I., S. Tristram-Nagle, D. Harries, N. Kucerka, J. F. Nagle, and V. A. Parsegian. 2006. Swelling of phospholipids by monovalent salt. *J. Lipid Res.* 47:302–309.

25. Petrache, H. I., T. Zemb, L. Belloni, and V. A. Parsegian. 2006. Salt screening and specific ion adsorption determine neutral-lipid membrane interactions. *Proc. Natl. Acad. Sci. USA.* 103:7982–7987.

26. Kharakoz, D. P. 2001. Phase-transition-driven synaptic exocytosis: a hypothesis and its physiological and evolutionary implications. *Biosci. Rep.* 21:801–830.

27. Parsegian, V. A., and R. P. Rand. 1995. Interaction in membrane assemblies. *In* Structure and Dynamics of Membranes. R. Lipowsky and E. Sackmann, editors. North-Holland, Amsterdam. 643–690.

28. Kunz, W., J. Henle, and B. W. Ninham. 2004. 'Zur Lehre von der Wirkung der Salze' (about the science of the effect of salts): Franz Hofmeister's historical papers. *Curr. Opin. Colloid Interface Sci.* 9: 19–37.

29. Lipowsky, R. 1995. Generic interactions of flexible membranes. In Structure and dynamics of membranes. R. Lipowsky, and E. Sackmann, editors. North-Holland, Amsterdam. 521–602.

30. Helfrich, W. 1978. Steric interaction of fluid membranes in multilayer systems. *Z. Naturforsch.* 33a:305–315.

31. Koynova, R., and M. Caffrey. 1998. Phases and phase transitions of the phosphatidylcholines. *Biochim. Biophys. Acta.* 1376:91–145.

32. Pabst, G., M. Rappolt, H. Amenitsch, and P. Laggner. 2000. Structural information from multilamellar liposomes at full hydration: full q-range fitting with high quality x-ray data. *Phys. Rev. E.* 62:4000–4009.

33. Pabst, G., R. Koschuch, B. Pozo-Navas, M. Rappolt, K. Lohner, and P. Laggner. 2003. Structural analysis of weakly ordered membrane stacks. *J. Appl. Crystallogr.* 63:1378–1388.

34. Pabst, G. 2006. Global properties of biomimetic membranes: perspectives on molecular features. *Biophys. Rev. Lett.* 1:57–84.

35. Pabst, G., J. Katsaras, V. A. Raghunathan, and M. Rappolt. 2003. Structure and interactions in the anomalous swelling regime of phospholipid bilayers. *Langmuir.* 19:1716–1722.

36. Caillé, A. 1972. Remarques sur la diffusion des rayons X dans les smectiques A. *C. R. Acad. Sc. Paris B.* 274:891–893.

37. De Gennes, P. G., and J. Prost. 1993. The Physics of Liquid Crystals. Oxford University Press, Oxford, UK.

38. Sun, W. J., R. M. Suter, M. A. Knewtson, C. R. Worthington, S. Tristram-Nagle, R. Zhang, and J. F. Nagle. 1994. Order and disorder in fully hydrated unoriented bilayers of gel phase dipalmitoylphosphatidylcholine. *Phys. Rev. E.* 49:4665–4676.

39. Strancar, J., T. Koklic, and Z. Arsov. 2003. Soft picture of lateral heterogeneity in biomembranes. *J. Membr. Biol.* 196:135–146.

40. Strancar, J., T. Koklic, Z. Arsov, B. Filipic, D. Stopar, and M. A. Hemminga. 2005. Spin label EPR-based characterization of biosystem complexity. *J. Chem. Inf. Model.* 45:394–406.

41. Arsov, Z., and J. Strancar. 2005. Determination of partition coefficient of spin probe between different lipid membrane phases. *J. Chem. Inf. Model.* 45:1662–1671.

42. Laggner, P., and H. Stabinger. 1976. The partial specific volume changes involved in the thermotropic phase transitions of pure and mixed lecithins. *In* Colloid and Interface Science. M. Kerker, editor. Academic Press, New York. 91–96.

43. Schnedlitz, D., T. Kenner, H. Heimel, and H. Stabinger. 1989. A sound-speed sensor for the measurement of total protein concentration in disposable, blood-perfused tubes. *J. Acoust. Soc. Am.* 86:2073–2080.

44. Hianik, T., M. Haburcák, K. Lohner, E. Prenner, F. Paltauf, and A. Hermetter. 1998. Compressibility and density of lipid bilayers composed of polyunsaturated phospholipids and cholesterol. *Colloids and Surfaces A.* 139:189–197.

45. Halstenberg, S., T. Heimburg, T. Hianik, U. Kaatze, and R. Krivanek. 1998. Cholesterol-induced variations in the volume and enthalpy fluctuations of lipid bilayers. *Biophys. J.* 75:264–271.

46. Sarvazyan, A. P. 1982. Development of methods of precise ultrasonic measurements in small volumes of liquids. *Ultrasonics.* 20:151–154.

47. Sarvazyan, A. P. 1991. Ultrasonic velocimetry of biological compounds. *Annu. Rev. Biophys. Biophys. Chem.* 20:321–342.

48. Rappolt, M., P. Laggner, and G. Pabst. 2004. Structure and elasticity of phospholipid bilayers in the Lα phase: A comparison of phosphatidylcholine and phosphatidylethanolamine membranes. *In* Recent Research Developments in Biophysics. S. G. Pandalai, editor. Transworld Research Network, Kerala, India. 363–394.

49. Pincus, P. A., and S. A. Safran. 1998. Charge fluctuations and membrane attractions. *Europhys. Lett.* 42:103–108.

50. Lau, A. W. C., and P. Pincus. 2002. Counterion condensation and fluctuation-induced attraction. *Phys. Rev. E.* 66:041501.

51. Dean, D. S., and R. R. Horgan. 2002. Electrostatic fluctuations in soap films. *Phys. Rev. E.* 65:061603.

52. Li, Y., and B. Y. Ha. 2004. Nonzero ionic size and charge-correlation forces between fluid membranes. *Phys. Rev. E.* 70:061503.

53. Petrache, H. I., N. Gouliaev, S. Tristram-Nagle, R. T. Zhang, R. M. Suter, and J. F. Nagle. 1998. Interbilayer interactions from high-resolution x-ray scattering. *Phys. Rev. E.* 57:7014–7024.

54. Mennicke, U., D. Constantin, and T. Salditt. 2006. Structure and interaction potentials in solid-supported lipid membranes studied by X-ray reflectivity at varied osmotic pressure. *Eur. Phys. J. E.* 20:221–230.

55. Liu, Y., and J. F. Nagle. 2004. Diffuse scattering provides material parameters and electron density profiles of biomembranes. *Phys. Rev. E.* 69:040901.

56. Salditt, T. 2005. Thermal fluctuations and stability of solid-supported lipid membranes. *J. Phys. Condens. Matter.* 17:R287–R314.

57. Greenwood, A. I., S. Tristram-Nagle, and J. F. Nagle. 2006. Partial molecular volumes of lipids and cholesterol. *Chem. Phys. Lipids.* 143: 1–10.

58. Mitaku, S., and K. Okano. 1981. Ultrasonic measurements of two-component lipid bilayer suspensions. *Biophys. Chem.* 14:147–158.

59. Mitaku, S., and T. Date. 1982. Anomalies of nanosecond ultrasonic relaxation in the lipid bilayer transition. *Biochim. Biophys. Acta.* 688: 411–421.

60. Aruga, S., R. Kataoka, and S. Mitaku. 1985. Interaction between Ca2+ and dipalmitoylphosphatidylcholine membranes. I. Transition anomalies of ultrasonic properties. *Biophys. Chem.* 21:265–275.

61. Colotto, A., D. P. Kharakoz, K. Lohner, and P. Laggner. 1993. Ultrasonic study of melittin effects on phospholipid model membranes. *Biophys. J.* 65:2360–2367.

62. Kharakoz, D. P., A. Colotto, K. Lohner, and P. Laggner. 1993. Fluid-gel interphase line tension and density fluctuations in dipalmitoylphosphatidylcholine multilamellar vesicles. An ultrasonic study. *J. Phys. Chem.* 97:9844–9851.

63. Kharakoz, D. P., and E. A. Shlyapnikova. 2000. Thermodynamics and kinetics of the early steps of solid-state nucleation in the fluid lipid bilayer. *J. Phys. Chem. B.* 104:10368–10378.

64. Dimova, R., B. Pouligny, and C. Dietrich. 2000. Pretransitional effects in dimyristoylphosphatidylcholine vesicle membranes: optical dynamometry study. *Biophys. J.* 79:340–356.

65. Lee, C. H., W. C. Lin, and J. Wang. 2001. All-optical measurements of the bending rigidity of lipid-vesicle membranes across structural phase transitions. *Phys. Rev. E.* 64:020901.